Thermalization of a UV laser ablation plume in a background gas: From a directed to a diffusionlike flow

Salvatore Amoruso
Coherentia-INFM, and INFM Unitá di Napoli, Dipartimento di Scienze Fisiche, Università di Napoli Federico II, Complesso Universitario di Monte S. Angelo, Via Cintia, I-80126 Napoli, Italy

Bo Toftmann and Jørgen Schou*
OPL, Risø National Laboratory, DK-4000 Roskilde, Denmark
(Received 16 January 2003; revised manuscript received 3 November 2003; published 14 May 2004)

Combined diagnostic measurements of deposition rates and ion time-of-flight signals have been employed to study the expansion of a laser ablation plume into a background gas. With increasing gas pressure the angular distribution of the collected ablated atoms becomes broader, while the total collected yield decreases. The total collected yield shows three separate regimes with increasing pressure, a vacuumlike regime, a transition regime with increasing plume broadening and splitting of the ion signal, and at the highest pressure a diffusionlike regime with a broad angular distribution. In the high-pressure regime the expansion can be described by a simple model based on diffusion from a confined plume.

DOI: 10.1103/PhysRevE.69.056403 PACS number(s): 52.38.Mf, 79.20.Ds, 81.15.Fg

I. INTRODUCTION

The expansion of a laser ablated plasma into a low-pressure background gas leads to complicated interactions. The production of a plasma plume from a solid target by impact of ultraviolet (uv) nanosecond laser pulses is not yet fully understood even for the simple case of a solid irradiated by a laser pulse in vacuum [1–5]. The subsequent propagation of the partly ionized plasma plume in the background gas is a complex phenomenon as well [1–3,6,7]. Even though many fundamental physical features have not yet been explored adequately, a number of important techniques, e.g., laser processing of solids and film production by pulsed laser deposition (PLD), are based on these interactions [1,8,9]. It is of great importance to know the dynamics of a plume of ablated material in a background gas in order to optimize the experimental parameters during a film production process.

Initially, the irradiation with a nanosecond laser pulse produces a thin layer of a partly ionized plasma on the target surface. Since the pressure of this plume is much higher than that of a typical background gas, the plume will expand rapidly, until the driving pressure has decreased considerably [10,11]. Spectroscopic measurements show that the plume is moving into the background gas with a confined spatial structure [7,11–15], but also that a fast component of the ablated material is transmitted through low-pressure background gases with little or no delay compared with vacuum [6,12,13]. Eventually, the confined part of the plume stops as a result of energy loss to shock wave formation, and the plume particles become thermalized [15–20]. The splitting of the plume ions and neutrals into a fast and slow component has been treated comprehensively [6,12,13,15,21–25], but except for few studies [15,24], only the ionic component has been investigated.

In this work we have performed combined measurements of deposition rates and ion signals which allow us to follow an ablated plume from the initial formation to the thermalization. In addition, we have identified three distinct pressure regimes, each of which is characterized by a particular behavior of the plume: (a) a vacuumlike regime at low pressure, (b) a transition regime with plume splitting and shock wave formation, and (c) a regime characterized by a diffusion of the ablated particles away from the plume at high pressure. In contrast to many earlier measurements, which have been carried out for complicated materials such as high T_c superconductors [1,12,26,27] or PZT (lead zirconate titanate) metal oxides [26,28], we have studied ablation for a simple one-component system, silver, into an atmosphere of oxygen and the chemically inert gases argon or xenon. Oxygen is a standard gas for PLD of metal oxides, but since chemical reactions between the plume atoms and the background gas atoms/molecules may occur, the results from a plume expansion in inert gases give a clearer picture of the expansion dynamics in a gas. The analysis is based partly on angular resolved measurements of the deposition from a silver plume as a function of background pressure, which in itself is an important result for the plume propagation. There is a clear broadening of the plume with increasing pressure for all gases [26] except for heavy target atoms in lighter gases [29–31].

II. EXPERIMENT

The measurements were carried out at the existing setup at Risø National Laboratory [4,5,32]. A frequency-tripled Nd:YAG (yttrium aluminum garnet) laser at 355 nm was directed at normal incidence onto a metal target in a chamber with a base pressure of 10^{-7} mbar. The duration of the laser pulse was 6 ns and the fluence was 2.5 J/cm^2 (corresponding to an intensity of 4×10^8 W/cm^2). The area of the circular laser beam spot was 0.04 cm^2. The angular distribution of

*Corresponding author. Email address: j.schou@risoe.dk

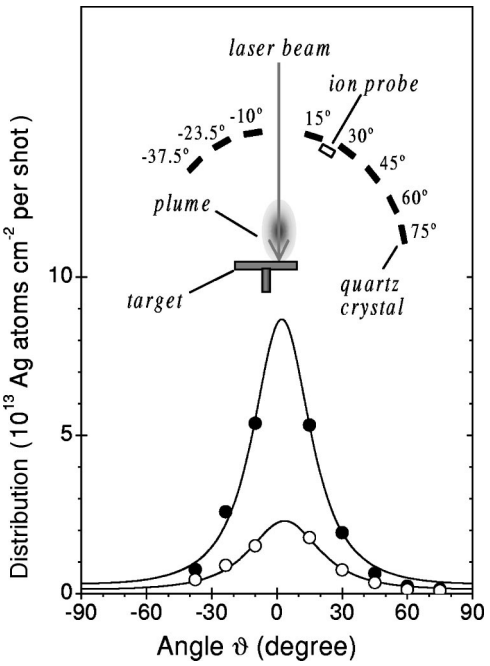

FIG. 1. Upper part, the experimental setup; lower part, angular distribution of the ablated Ag particles as a function of angle with respect to the normal. Closed circles, 3.9×10^{-6} mbar; open circles, 5.4×10^{-2} mbar. The curves are fits to Eq. (1) with $k_z=3.0\pm0.2$ (closed circles) and $k_z=2.5\pm0.2$ (open circles). Fluence: 2.5 J/cm^2.

the ablated flux of both neutrals and ions was measured *in situ* 80 mm from the target using a circular array of eight quartz crystal microbalances (QCMs) in the horizontal plane as shown in Fig. 1. The crystals were located at 10°, 15°, 23.5°, 30°, 37.5°, 45°, 60°, and 75° with respect to the surface normal, and each crystal had a 6 mm diameter active area. The accuracy of the measurements was about 0.1 Hz corresponding to 1.2×10^{13} Ag atoms/cm^2. Each run was taken on a fresh target spot, typically with 200–1000 pulses at a repetition rate of 0.1 Hz and with a subsequent relaxation time for the crystals of 4–6 h. The planar Langmuir probe was a 2×2 mm^2 square copper plate insulated on the rear side similar to the probes in Ref. [4]. The probe was oriented to face the target spot and placed 75 mm from the target with an angle of 20° with respect to the normal. A few measurements were repeated for a probe angle of 3° with respect to the normal. During the ion collection the probe was biased at −10 V.

The laser incidence along the normal and the circular beam spot mean that the plume is rotationally symmetric with respect to the normal [33]. Thus we can determine the total number of ablated atoms by integrating over the full hemisphere. The drawback by this geometry is that we cannot measure the outgoing flow in a small solid angle around the normal of the target.

III. RESULTS AND DISCUSSION

A. The angular distribution

Figure 1 shows the angular distributions of the collected Ag atoms in vacuum and in a low-pressure argon background gas. The values of the collected yield for ablation in a background gas are considerably lower than that in vacuum. In both cases the distribution is peaked strongly in forward direction. The data have been fitted with the angular distribution $F(\theta)$ from Anisimov's model [10,34,35]:

$$F(\theta)/F(0) = (1+\tan^2\theta)^{3/2}[1+k_z^2\tan^2\theta]^{-3/2}, \qquad (1)$$

where the fitting parameter $k_z=Z_{inf}/X_{inf}$ is the ratio of the limiting value of the cloud front along the Z axis (in forward direction into vacuum) and the value of the front in horizontal direction along the X axis. This distribution accounts for the deposition per unit area on a hemisphere in contrast to the expressions indicated in Ref. [34]. In Anisimov's model the gas plume expands in vacuum as a self-similar ellipsoidal cloud based on a system of hydrodynamic equations. Strictly speaking, the theory works only for a neutral gas plume, but we have been encouraged to use it also for an expanding plasma in view of the good agreement with our data for the ion flow from a silver plume in vacuum [35].

Previously, Eq. (1) has been used for the analysis of deposition measurements in a background gas as well [28]. This is also confirmed by the good agreement between the fit for a realistic value of k_z and the data points for ablation in the background gas in Fig. 1. Other measurements indicate that Eq. (1) is also a good approximation for the distribution at values close to 0° [28,35]. For the fluence used here sputtering of the deposit on the collectors plays only a minor role [5,36].

The full width at half maximum $\Delta\theta$ of the angular distribution can be found directly from the fitting parameter k_z:

$$\Delta\theta = 2\ \arctan[(2^{2/3}-1)(k_z^2-2^{2/3})]^{1/2}. \qquad (2)$$

In Fig. 2(a), the angular distribution of the collected yield in an argon background gas has been shown. The distribution for all pressures has been normalized to the maximum value for reasons of clarity. The width $\Delta\theta$ of the collected ablation yield is shown in Fig. 2(b). For pressure values up to 1×10^{-2} mbar there is no noticeable change in the distribution [regime (a)]. Then between 1×10^{-2} and 2×10^{-1} mbar [regime (b)] $\Delta\theta$ changes from 30° to 80° as a result of the increasing number of collisions between the ablated Ag atoms and the Ar atoms in the background gas. For higher pressure ($\geqslant2\times10^{-1}$ mbar) up to the upper limit studied in this work the broadening does not increase significantly from $\Delta\theta\cong80°$ [regime (c)]. A similar plot of the distribution of silver atoms in an oxygen gas is shown in Fig. 3. Essentially, the distribution shows the same trend as that in argon, even though the mass of the scattering gas molecules is somewhat lower for oxygen than the atomic mass of argon. This demonstrates that the effect of chemical reactions between the silver atoms and the oxygen molecules during the plume expansion is comparatively small.

B. Time-of-flight distributions and integrated yields

The three pressure regimes are also clearly visible in the total collected yield of Ag atoms obtained by integrating Eq. (1) over the full hemisphere (Fig. 4, lower part). This number

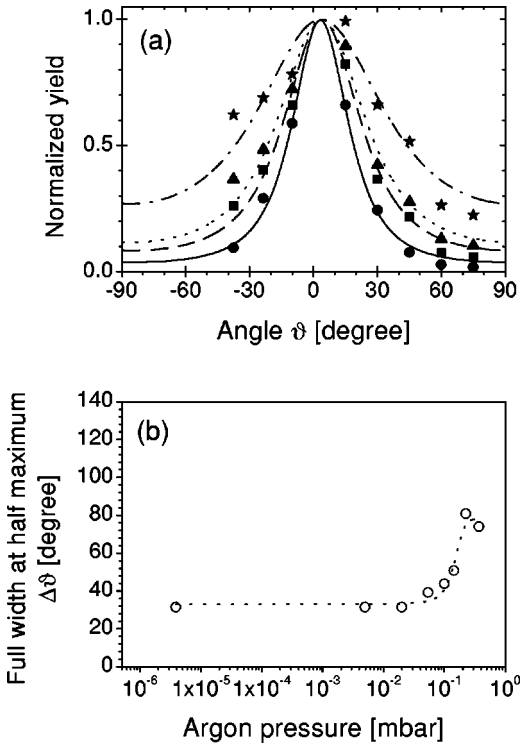

FIG. 2. Upper part: angular distribution of the collected ablation yield as a function of argon pressure. The distribution has been normalized to the maximum. The curves are fits to Eq. (1). For Argon: (●) 2.0×10^{-2} mbar; (■) 1.0×10^{-1} mbar; (▲) 1.5×10^{-1} mbar; (♠) 2.3×10^{-1} mbar. Lower part: The full width at half maximum $\Delta\theta$ of the angular distribution of the collected Ag atoms as a function of Ar background pressure. The dashed line has been inserted to guide the eye. Fluence: 2 J/cm^2.

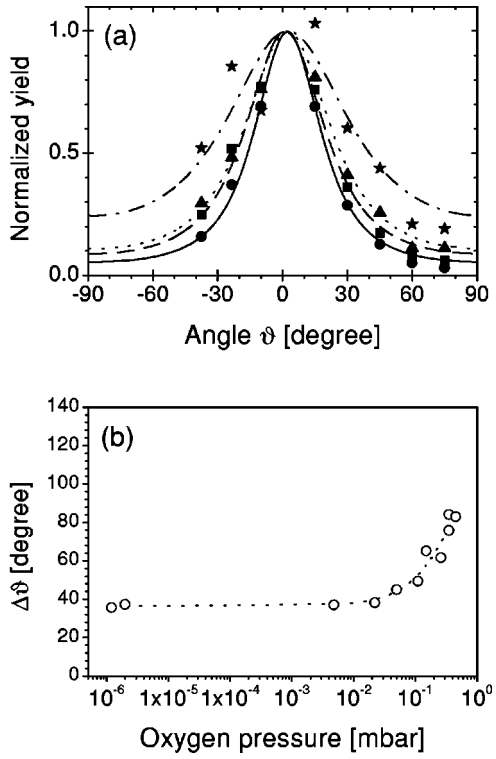

FIG. 3. Upper part: angular distribution of the collected ablation yield as a function of oxygen pressure. The distribution has been normalized to the maximum. The curves are fits to Eq. (1). For Oxygen: (●) 4.8×10^{-3} mbar; (■) 5.0×10^{-2} mbar; (▲) 1.1×10^{-2} mbar; (♠) 3.5×10^{-1} mbar. Lower part: The full width at half maximum $\Delta\theta$ of the angular distribution of the collected Ag atoms as a function of O_2 background pressure. The dashed line has been inserted to guide the eye. Fluence: 2.5 J/cm^2.

is essentially constant and equal to the vacuum yield for pressures up to $\approx1\times10^{-2}$ mbar [regime (a)], the yield of collected atoms decreases strongly up to $\approx2\times10^{-1}$ mbar [regime (b)], and finally it falls off exponentially for high pressure [regime (c)].

Each regime can be characterized by an ion probe signal (upper part of Fig. 4). In the time-of-flight (TOF) signal for regime (a) the vacuum signal becomes slightly broadened by few collision processes in the gas. In regime (b) the increasing number of collisions means that a substantial fraction of the Ag atoms are retarded and form a slowed, second peak. This peak splitting continues until only the slow peak remains visible in the ion signal at high pressure in regime (c). These TOF spectra were taken at an angle of 20°, but a control series at 3° showed a similar behavior except for the absolute magnitude of the signals. The dynamics of the silver ions in argon and in oxygen is similar to that described by Geohegan for a yttrium plume expanding in oxygen [12] and Wood *et al.* [6,23] for a silicon plume in argon background gas.

The ions comprise a significant part of the total particles in the silver plume [35,36], and the TOF signal is, therefore, also representative of the total flow measured as a deposit on the crystals. This surprising feature is actually seen in the lower part of Fig. 4, in which the time-integrated TOF signal has been plotted together with the total collected ablation yield. The ion yield exhibits the same behavior with pressure as the total collected yield over many orders of magnitude. Since the ionization potential of Ag atoms (7.6 eV) is much less than that of Ar (15.8 eV), the probability of ionization of the gas atoms by charge transfer is small. Thus the peaks in the TOF spectra consist primarily of Ag^+ ions. However, one may not exclude a minor fraction of collisionally excited Ar^+ ions. The observation that silver ions are dominant in the plume agrees completely with the analysis of Wood *et al.* [6,23] who did not include ionized background gas atoms in their analysis either.

C. Diffusion and thermalization of the plume particles

In regime (c) the plume particles of the second peak, which have not been transmitted through the background gas, form a confined, spherelike structure [14]. Eventually, the silver atoms escape from the slowly moving plume by diffusion through the background gas. We have approximated the plume as a homogeneous spherical source with radius a (Fig. 5) and determined the flux $J(t)$ on a hemispherical shell in a distance R from the target by solving the diffusion equation [37]. The total collected yield for $a \ll R$ is obtained by the integral over the time t,

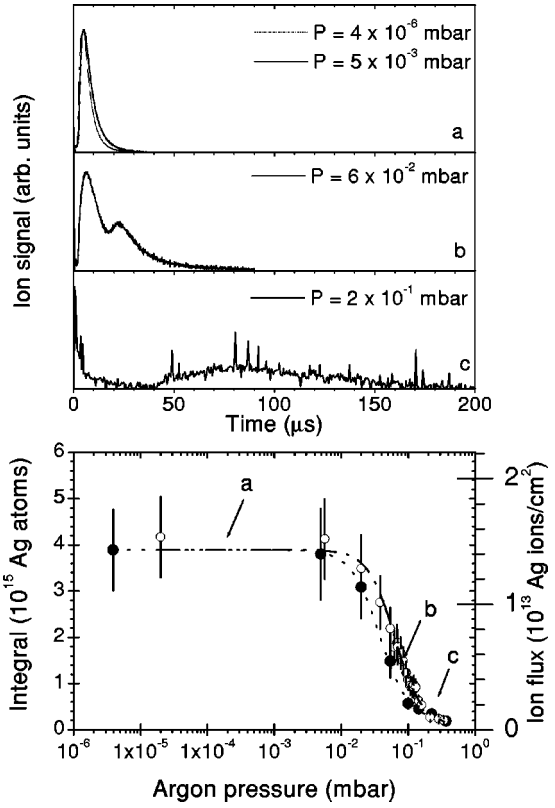

FIG. 4. Upper part: (a) Two ion signals in pressure regime (a), see lower part of the figure. (b) Ion signal in regime (b), (c) ion signal in regime (c). All signals collected with the planar probe at 20° from the normal in the distance of 75 mm from the target. Fluence: 2.5 J/cm^2. Lower part: total collected yield of Ag atoms (closed circles, dotted curve, left axis). The collected yield has been obtained from an integration of Eq. (1) over the full hemisphere. Time-integrated ion yield from the probe (open circles, dashed curve, right axis) as a function of the Ar pressure normalized to the total collected yield for "vacuum." The ion yield has been obtained by integrating the ion signals in the upper part with respect to time. Fluence: 2.5 J/cm^2.

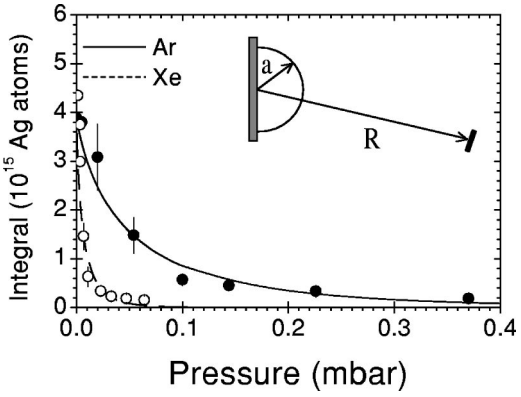

FIG. 5. Total collected yield (as in Fig. 4, lower part) as a function of Ar (closed circles) and Xe (open circles) pressure. The curves are fits to Eq. (3) with τ=3.4 ms (Ar) and τ=0.9 ms (Xe). The inset shows the geometry for Eq. (3).

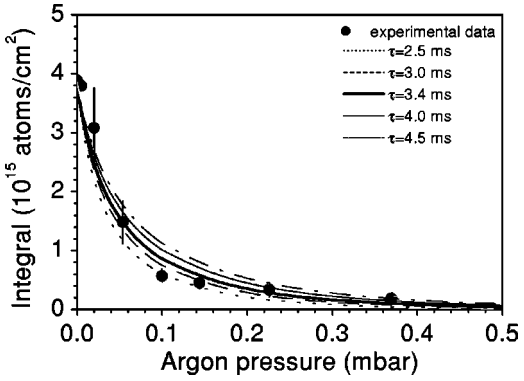

FIG. 6. Fits of the total collected yield in an Ar background gas to Eq. (3) with τ as a parameter. The data are from Fig. 5.

$$Y(a) = 2\pi R^2 \int_0^\infty J(t)\exp\left(-\frac{t}{\tau}\right)dt, \tag{3}$$

where

$$J(t) = \frac{C_0 R}{16(\pi k)^{3/2} t^{5/2}} e^{-R^2/4kt}\left[1 + \frac{\left(\frac{R^2}{kt} - 10\right)a^2}{40kt}\right]. \tag{4}$$

C_0 accounts for the flux in vacuum, k the diffusivity of the background gas ($k = 1/3\langle \nu_{th}\rangle \lambda$, where $\langle \nu_{th}\rangle$ and λ are the thermal speed and mean free path, respectively [37]). τ is the time constant of the drain from the plume, which accounts for the loss of plume particles from pumping of the system and deposition on the chamber surfaces [38].

Since deviations from the free plume expansion occur when the mass of the adjacent background gas at the plume periphery becomes comparable with the plume mass M_p [39], the radius of the hemispherical plume a is determined by the relation $2/3\ \pi\rho_g a^3 \approx M_p$. In terms of the background gas pressure P this gives

$$a = \sqrt[3]{\frac{3}{2\pi}\frac{M_p k_B T_g}{m_g}} P^{-1/3}, \tag{5}$$

where k_B is the Boltzmann constant and ρ_g, T_g, and m_g are the density, the temperature, and the atomic mass of the ambient gas. Equation (3) has been fitted to the total collected yield in Fig. 5 with τ as the only adjustable parameter. There is very good agreement between the yield in Ar and Eq. (3) (τ=3.4 ms) as well as that in Xe (τ=0.9 ms). For oxygen (not shown in the figure) the value is close to that of argon (τ=3.5 ms). As seen in Fig. 6 the shape of the curve depends strongly on τ, but not on a which is a much less sensitive parameter for the diffusion treatment. The analysis does provide us with fairly accurate values of τ which is a specific quantity for each vacuum setup, i.e., determined by the pumping speed or by the area of all collecting surfaces near the ablation volume. The order of magnitude of the time constant τ is larger than, but also in reasonable agreement with the TOF values deduced from Fig. 4(c). The small value of τ for the xenon background gas reflects the point that the diffusion of silver atoms in a heavy gas as xenon is slow

compared with that for argon, so that the Ag atoms in xenon have a larger probability of being pumped away before reaching the QCM collectors.

The validity of this diffusion approach clearly does have certain limitations, since the angular distribution of the collected yield at high pressures is not isotropic, but weakly peaked in forward direction. This discrepancy clearly reflects the fact that the initial "vacuum" distribution is strongly peaked in forward direction rather than isotropic and that the plume atoms along the normal have the highest energy, e.g., up to more than 200 eV [4,40]. The scattering cross section at these plume energies is not well known, and the mean free path may be considerably enhanced for fast ablated atoms [19].

The plume splitting of the ions occurs in the transition regime (b) and is accompanied by significant reduction of the total collected yield. In this regime a typical (energy-independent) cross section of 5×10^{-16} cm^2 [6] leads to five to ten collisions on a trajectory from the target to the QCMs. In the diffusionlike regime (c) a particle moving a distance corresponding to that between the target and the QCMs would suffer more than 30 collisions. The many collisions can easily reduce an initial energy, e.g., 50 eV, of an atom to a value below the thermalization limit (<0.1 eV) [20].

IV. CONCLUSION

In summary, we have identified three pressure regimes for the plume expansion and thermalization in a background gas. A low-pressure "vacuumlike" regime (a) with a flow in forward direction and with only little scattering of the ablated atoms. Then a transition regime (b) with a pronounced broadening of the angular distribution occurs as a result of strong momentum transfer to the background gas. In this regime the ion probe signal splits into two peaks, of which the fast one consists of atoms which have suffered few collisions with the background gas atoms. Also shock wave formation is important in this regime, but this feature has not been directly observed in the present work. Finally, at the highest pressure in regime (c) the broadening of the angular distribution reaches $\Delta\theta\cong80°$, and only the slow peak of thermalizing atoms in the ion signal has survived at the probe position. This regime is characterized by a diffusion of the slow particles from the confined plume to the QCM collectors. The total collected ablation yield can be determined from the diffusion equation for a simple geometry with a single adjustable parameter, a time constant τ which accounts for the drain of ablated particles out of the collector system. The transition pressure from one regime to another depends strongly on the specific gas.

ACKNOWLEDGMENTS

This work was supported by the EU Growth Programme under Contract No. G6RD-CT1999-00084 and by the Danish Natural Science Research Council.

[1] D. H. Lowndes, in *Laser Ablation and Desorption*, edited by J. C. Miller and R. F. Haglund, Experimental Methods in the Physical Sciences Vol. 30 (Academic, New York, 1998), p. 475.
[2] P. R. Willmott and J. R. Huber, Rev. Mod. Phys. **72**, 315 (2000).
[3] S. Amoruso, R. Bruzzese, N. Spinelli, and R. Velotta, J. Phys. B **32**, R131 (1999).
[4] B. Toftmann, J. Schou, T. N. Hansen, and J. G. Lunney, Phys. Rev. Lett. **84**, 3998 (2000).
[5] B. Toftmann, J. Schou, and J. G. Lunney, Phys. Rev. B **67**, 104101 (2003).
[6] R. F. Wood, K. R. Chen, J. N. Leboeuf, A. A. Puretzky, and D. B. Geohegan, Phys. Rev. Lett. **79**, 1571 (1997).
[7] T. E. Itina, J. Hermann, P. Delaporte, and M. Sentis, Phys. Rev. E **66**, 066406 (2002).
[8] D. Bäuerle, *Laser Processing and Chemistry*, 3rd ed, (Springer, Berlin, 2000).
[9] *Pulsed Laser Deposition of Thin Films*, edited by D. B. Chrisey and G. B. Hubler (Wiley-Interscience, New York, 1994).
[10] S. I. Anisimov, B. S. Luk'yanchuk, and A. Luches, Appl. Surf. Sci. **96-98**, 24 (1996).
[11] S. Proyer and E. Stangl, Appl. Phys. **60**, 573 (1995).
[12] D. B. Geohegan, Thin Solid Films **220**, 138 (1992).
[13] D. B. Geohegan and A. A. Puretzky, Appl. Phys. Lett. **67**, 197 (1995).
[14] Y. Nakata, H. Kalbara, T. Okada, and M. Maeda, J. Appl. Phys. **80**, 2458 (1996).
[15] S. Amoruso, B. Toftmann, J. Schou, R. Velotta, and X. Wang, Thin Solid Films **453-454**, 562 (2004).
[16] S. Amoruso, R. Bruzzese, N. Spinelli, R. Velotta, M. Vitiello, and X. Wang, Phys. Rev. B **67**, 224503 (2003).
[17] N. Arnold, J. Gruber, and J. Heitz, Appl. Phys. A: Mater. Sci. Process. **69**, S87 (1999).
[18] B. Y. Man, X. T. Wang, and A. H. Liu, J. Appl. Phys. **83**, 3509 (1998).
[19] T. E. Itina, W. Marine, and M. Autric, J. Appl. Phys. **82**, 3536 (1997).
[20] G. M. Turner, I. S. Falconer, B. W. James, and D. R. McKenzie, J. Appl. Phys. **65**, 3671 (1989).
[21] T. N. Hansen, J. Schou, and J. G. Lunney, Appl. Surf. Sci. **138-139**, 184 (1999).
[22] B. Thestrup, B. Toftmann, J. Schou, B. Doggett, and J. G. Lunney, Appl. Surf. Sci. **208-209**, 33 (2003).
[23] R. F. Wood, J. N. Leboeuf, D. B. Geohegan, A. A. Puretzky, and K. R. Chen, Phys. Rev. B **58**, 1533 (1998).
[24] S. S. Harilal, C. V. Bindhu, M. S. Tillack, F. Najmabadi, and A. C. Gaeris, J. Appl. Phys. **93**, 2380 (2003).
[25] S. S. Harilal, C. V. Bindhu, M. S. Tillack, F. Najmabadi, and A. C. Gaeris, J. Phys. D **35**, 2935 (2002).
[26] K. L. Saenger, in *Laser Processing and Chemistry* (Ref. [9]), p. 199.
[27] J. Gonzalo, F. Vega, and C. N. Afonso, J. Appl. Phys. **77**, 6588

(1995).
[28] M. Tyunina, J. Wittborn, C. Björmander, and K. V. Rao, J. Vac. Sci. Technol. A **16**, 2381 (1998).
[29] S. Amoruso, B. Toftmann, and J. Schou (unpublished).
[30] T. Szörenyi and J. M. Ballesteros, Appl. Surf. Sci. **109-110**, 327 (1997).
[31] D. J. Lichtenwalner, O. Auciello, R. Dat, and A. I. Kingdon, J. Appl. Phys. **74**, 7497 (1993).
[32] W. Svendsen, J. Schou, T. N. Hansen, and O. Ellegaard, Appl. Phys. A: Mater. Sci. Process. **66**, 493 (1998).
[33] T. E. Itina, A. A. Katassonov, W. Marine, and M. Autric, J. Appl. Phys. **83**, 6050 (1998).
[34] S. I. Anisimov, D. Bäuerle, and B. S. Luk'yanchuk, Phys. Rev. B **48**, 12 076 (1993).
[35] B. Thestrup, B. Toftmann, J. Schou, B. Doggett, and J. G. Lunney, Appl. Surf. Sci. **197-198**, 175 (2002).
[36] S. Fähler, K. Sturm, and H.-U. Krebs, Appl. Phys. Lett. **75**, 3766 (1999).
[37] H. S. Carslaw and J. C. Jaeger, *Conduction of Heat in Solids* (Oxford, Clarendon, 1959).
[38] *Classical Kinetic Theory of Fluids*, edited by M. Dee Leener and P. Resibois (Wiley, New York, 1977).
[39] Ya. B. Zel'dovich and Yu. P. Raizer, *Physics of Shock Waves and High-Temperature Hydrodynamic Phenomena* (Academic, New York, 1966).
[40] T. N. Hansen, J. Schou, and J. G. Lunney, Appl. Phys. Lett. **72**, 1829 (1998).